

Journal of Visualized Experiments

Time-resolved, dynamic computed tomography angiography for characterization of aortic endoleaks and for treatment guidance via 2D3D fusion-imaging.

--Manuscript Draft--

Article Type:	Invited Methods Collection - JoVE Produced Video
Manuscript Number:	JoVE62958R3
Full Title:	Time-resolved, dynamic computed tomography angiography for characterization of aortic endoleaks and for treatment guidance via 2D3D fusion-imaging.
Corresponding Author:	Marton Berczeli UNITED STATES
Corresponding Author's Institution:	
Corresponding Author E-Mail:	marton.berczeli@gmail.com
Order of Authors:	Marton Berczeli Ponraj Chinnadurai Su Min Chang Alan B. Lumsden
Additional Information:	
Question	Response
Please specify the section of the submitted manuscript.	Medicine
Please indicate whether this article will be Standard Access or Open Access.	Standard Access (\$1400)
Please indicate the city, state/province, and country where this article will be filmed . Please do not use abbreviations.	Houston, Texas, USA
Please confirm that you have read and agree to the terms and conditions of the author license agreement that applies below:	I agree to the Author License Agreement
Please provide any comments to the journal here.	
Please confirm that you have read and agree to the terms and conditions of the video release that applies below:	I agree to the Video Release

TITLE:

Time-Resolved, Dynamic Computed Tomography Angiography for Characterization of Aortic Endoleaks and Treatment Guidance *via* 2D-3D Fusion-Imaging

AUTHORS AND AFFILIATIONS:

Marton Berczeli^{1,2*}, Ponraj Chinnadurai^{1,3}, Su Min Chang⁴, Alan B. Lumsden¹

¹Department of Cardiovascular Surgery, Houston Methodist Hospital, Tx, USA

²Department of Vascular and Endovascular Surgery, Semmelweis University, Budapest, Hungary

³Advanced Therapies, Siemens Medical Solutions USA Inc., Malvern, PA, USA

⁴Department of Cardiology, Houston Methodist Hospital, Houston, Tx, USA

Email addresses of the authors:

Marton Berczeli marton.berczeli@gmail.com, mtberczeli@houstonmethodist.org

Ponraj Chinnadurai pchinnadurai@houstonmethodist.org

Su Min Chang smchang@houstonmethodist.org

Alan B. Lumsden ablumsden@houstonmethodist.org

Email addresses of the corresponding author:

Marton Berczeli marton.berczeli@gmail.com, mtberczeli@houstonmethodist.org

KEYWORDS:

endovascular aneurysm repair, aortic endoleak, triphasic CT imaging, delayed CT imaging, dynamic CTA imaging, time-resolved CTA, EVAR, endoleak embolization, image fusion, post-EVAR surveillance

SUMMARY:

Dynamic computed tomography angiography (CTA) imaging provides additional diagnostic value in characterizing aortic endoleaks. This protocol describes a qualitative and quantitative approach using time-attenuation curve analysis to characterize endoleaks. The technique of integrating dynamic CTA imaging with fluoroscopy using 2D-3D image fusion is illustrated for better image guidance during treatment.

ABSTRACT:

In the United States, more than 80% of all abdominal aortic aneurysms are treated by endovascular aortic aneurysm repair (EVAR). The endovascular approach warrants good early results, but adequate follow-up imaging after EVAR is imperative to maintain long-term positive outcomes. Potential graft-related complications are graft migration, infection, fracture, and endoleaks, with the last one being the most common. The most frequently used imaging after EVAR is computed tomography angiography (CTA) and duplex ultrasound. Dynamic, time-resolved computed tomography angiography (d-CTA) is a reasonably new technique to characterize the endoleaks. Multiple scans are done sequentially around the endograft during acquisition that grants good visualization of the contrast passage and graft-related complications. This high diagnostic accuracy of d-CTA can be implemented into therapy *via* image fusion and

reduce additional radiation and contrast material exposure.

This protocol describes the technical aspects of this modality: patient selection, preliminary image review, d-CTA scan acquisition, image processing, qualitative and quantitative endoleak characterization. The steps of integrating dynamic CTA into intra-operative fluoroscopy using 2D-3D fusion-imaging to facilitate targeted embolization are also demonstrated. In conclusion, time-resolved, dynamic CTA is an ideal modality for endoleak characterization with additional quantitative analysis. It can reduce radiation and iodinated contrast material exposure during endoleak treatment by guiding interventions.

INTRODUCTION:

Endovascular aortic aneurysm repair (EVAR) has shown superior early mortality results than open aortic repair¹. The approach is less invasive but may result in higher mid to long-term re-intervention rates due to endoleaks, graft migration, fracture². Hence better EVAR surveillance is critical to achieving good mid to long-term results.

Current guidelines suggest the routine use of duplex ultrasound and triphasic CTA³. Dynamic, time-resolved computed tomography angiography (d-CTA) is a relatively new modality used for EVAR surveillance⁴. During d-CTA, multiple scans are acquired in different time points along the time attenuation curve after contrast injection, hence the term time-resolved imaging. This approach has shown better accuracy in characterizing endoleaks after EVAR than conventional CTA⁵. An advantage of time-resolved acquisition is the ability to quantitatively analyze the Hounsfield unit changes in a selected region of interest (ROI)⁶.

The additional benefit of accurately characterizing endoleaks with d-CTA is that the scan can be used for image fusion during interventions, potentially minimizing the need for further diagnostic angiography. Image fusion is a method when previously acquired images are overlaid onto real-time fluoroscopy images to guide endovascular procedures and subsequently reduce contrast agent consumption and radiation exposure^{7,8}. Image fusion in the hybrid operating room (OR) using a 3D dynamic CTA scan can be achieved by two approaches: (1) 3D-3D image fusion: where 3D d-CTA is fused with intraoperatively acquired non-contrast cone-beam CT images, (2) 2D-3D image fusion, where 3D d-CTA is fused with biplanar (anteroposterior and lateral) fluoroscopic images. 2D-3D image fusion approach has been shown to significantly lower the radiation compared with 3D-3D technique⁹.

This protocol describes the technical and practical aspects of dynamic CTA imaging for endoleak characterization and introduces a 2D-3D image fusion approach with d-CTA for intra-operative image guidance.

PROTOCOL:

This protocol follows the ethical standards of the national research committee and with the 1964 Helsinki declaration. This protocol is approved by Houston Methodist Research Institute.

1. Patient selection and prior image review

NOTE: Dynamic CTA imaging should be considered as a follow-up imaging modality in patients with increasing aneurysm size and endoleak after stent-graft implantation, persistent endoleak after interventions, or in patients with increasing aneurysms sac size without demonstrable endoleak. Like conventional CT imaging, this technique involves iodinated contrast injection that may be relatively contraindicated in patients with severe renal failure.

1.1. Before starting the actual scan, review the prior imaging studies for the presence of endoleak and stent-graft type.

NOTE: This can provide information to decide the scan range and temporal distribution during the image acquisition. The most commonly available imaging is the conventional CTA scans with bi-(non-contrast scan and arterial scan) or triple-phase (non-contrast scan, arterial scan, and delayed scan).

2. d-CTA Image acquisition

2.1. Position the patient in a supine position on the CT scanner table.

2.2. Gain peripheral venous access.

NOTE: Ensure that access is gained by visualizing the venous back bleeding.

2.3. Perform **Topogram** and **Non-Contrast CT Image Acquisition** using Sn-100 Tin filter (see **Table of Materials**) to reduce the radiation exposure and for the region of interest selection in the d-CTA scan.

NOTE: After the non-contrast scan, the location of the endograft will be visible. Place the region of interest just above the endograft.

2.4. Perform timing bolus⁶ to check the contrast arrival time by placing a region of interest above the stent graft in the abdominal aorta.

2.4.1. Inject 10-20 mL of the contrast (see **Table of Materials**) through the peripheral venous access, followed by 50 mL of saline injection at a 3.5–4 mL/min flow rate. Acquire timing bolus scan.

NOTE: Contrast arrival is recorded by the CT scanner (see **Table of Materials**) based on Hounsfield unit change inside the aorta⁶.

2.5. By selecting the DynMulti4D menu point in the pop-up “Cycle time window” plan the distribution and the number of scans based on the contrast arrival time from timing bolus and the findings from prior imaging studies.

NOTE: If type I endoleak is suspected, perform more scans on the early phase of the contrast enhancement curve that is given by the timing bolus. If type II endoleak is suspected, perform more scans on the later phase.

2.5.1. For type I endoleak, include more scans during the earlier phase of the time-attenuation curve (scan at every 1.5 s at the beginning and then every 3-4 s).

2.5.2. For type II endoleak that appear later, include more scans during the later phase of the time-attenuation curve.

2.5.3. If no prior imaging studies are available, distribute the scans equally around the peak of the time-attenuation curve.

2.6. Optimize imaging parameters, including kV, scan range, etc., to reduce radiation exposure. Use settings shown in **Table 1** for acquiring a dynamic scan with the CT scanner (see **Table of Materials**) used in this work.

2.7. Inject the contrast for d-CTA acquisition: 70-80 mL of the contrast material, followed by 100 mL of saline injections at a 3.5–4 mL/min flow rate through the peripheral access.

2.8. **Start** d-CTA image acquisition using the delay time based on the timing bolus described in step 2.4. Breath-hold is not necessary during acquisition, given that the duration of d-CTA image acquisition ranges from 30–40 s.

2.9. Send acquired, reconstructed images to Picture Archiving and Communication System (PACS) for qualitative and quantitative review of time-resolved angiographic images. To do this, select the data image and perform a mouse click on the bottom left side of the software.

3. Dynamic-CTA image analysis

3.1. Open the software (see **Table of Materials**) for reading the image. Search for the patient's name or identification number to find the acquired images. Select the acquired d-CTA images and process them using the **CT dynamic angio** workflow.

NOTE: The layout is shown in **Figure 1**.

3.2. Minimize respiratory motion artifacts between d-CTA images by selecting the dedicated software's **Align Body** motion correction menu item (**Figure 1**).

3.3. Qualitative analysis: Check axial slices of CT images when maximum opacification of the aorta occurs to interpret any obvious endoleak.

3.3.1. Then analyze scans in multiplanar reconstruction mode; if endoleak is suspected, focus on the endoleak and use the timescale shown in **Figure 1** to watch time-resolved images and

infer the source of endoleak.

3.4. Quantitative analysis: Click on the **Time Attenuation Curve (TAC)** function shown in **Figure 1**. Select a region above the stent-graft (ROI_{aorta}) and draw a circle using the TAC function, then select the endoleak (ROI_{endoleak}) region and draw a circle there as well.

NOTE: Target vessels can be selected (ROI_{target}) to determine the role of the vessel to the endoleak (inflow or outflow).

3.4.1. Analyze the acquired TAC (**Figure 2**) to determine the endoleak characteristics. Subtract the time to the peak value of the endoleak from the aortic ROI curves to get the Δ time to peak value. This value can be used for endoleak analysis⁶.

3.5. After qualitative and quantitative analysis, infer the type and source of endoleak.

NOTE: Type I endoleaks appear as parallel contrast enhancement next to the graft, usually because of the inadequate sealing zone and have a shorter time difference between the aortic and endoleak enhancement curves (Δ time to peak value) between aortic and endoleak ROI. Type II endoleaks are related to an inflow vessel with retrograde filling through collateral and have prolonged Δ time to peak value between aortic and endoleak ROI. Based on experience, a Δ time-to-peak value of higher than 4 s was not recorded for type I endoleaks.

4. Intra-operative image fusion guidance

4.1. Position the patient supine on the hybrid operating room (OR) table.

4.2. Load the selected dynamic CTA scan that has the best visibility of the endoleak in the hybrid OR workstation. Manually annotate critical landmarks on the scan: renal arteries ostia, internal iliac arteries ostia, endoleak cavity, lumbar artery(ies), or inferior mesenteric artery.

4.3. Select 2D-3D image fusion in the workstation and acquire an anteroposterior and an oblique fluoroscopic image of the patient using the 2D-3D image fusion workflow. For this, move the C-arm to the required angle(s) with the joystick on the operating table and step on the CINE acquisition pedal.

4.4. Electronically align the stent graft with markers from the 3D dynamic CTA scan with the fluoroscopic images using automated image registration, followed by manual refinement if necessary (**Figure 3**) in the 3D post-processing workstation (Drag one image for manual alignment). Check and accept the **2D-3D Image Fusion** and **Overlay** the markers from d-CTA on the real-time 2D fluoroscopic image (**Figure 4**).

4.5. Perform the endoleak embolization using the overlaid markers from d-CTA as guidance.

REPRESENTATIVE RESULTS:

The dynamic imaging workflow in two patients is illustrated here.

Patient I

An 82-year-old male patient with chronic obstructive pulmonary disease and hypertension had a previous infrarenal EVAR (2016). In 2020 the patient was referred from an outside hospital for a possible type I or type II endoleak based on conventional CTA. and an adjunctive endoanchor placement in 2020 for type Ia endoleak. Dynamic CTA was performed that diagnosed a type Ia endoleak, and the patient underwent proximal zone ballooning plus received endoanchors to gain more sealing zone for the graft. After the intervention, a dynamic control CTA was performed, acquiring 12 scans under 21 s scan time with 90 kV using 85 mL iodinated contrast material. Qualitative analysis showed a persisting type Ia endoleak illustrated in **Figure 5**. Quantitative TAC analysis showed a 12.2 s time to peak value for ROI_{aorta} and a 15.4 s to peak value for ROI_{endoleak} creating a 3.2 s time to a peak value (**Figure 6**). The patient received a fenestrated-EVAR; the procedure was done using 2D-3D image fusion during the procedure.

Patient II

A 62-year-old male patient with a medical history of obesity, stroke, renal insufficiency (creatinine: 2.02 mg/dL), hypertension, hyperlipidemia, and coronary artery disease. The patient received an infrarenal EVAR at an outside hospital in 2018. He was referred to our Institution for a possible type II endoleak on conventional CTA. Dynamic CTA was performed with acquiring 12 scans under 52 s at 100 kV using 70 mL iodinated contrast material. Sac enlargement with a type II endoleak was detected from bilateral L3 lumbar arteries as inflow vessels shown in **Figure 7**. Time attenuation curve analysis showed a 7.2 s time to peak value for ROI_{aorta} and 24.6 s for ROI_{endoleak} at the level of the L3 vertebra (**Figure 8**). An additional ROI was selected in the inferior portion of the sac, demonstrating the downward flow from the level of the bilateral lumbar arteries by the delayed time to a peak value (ROI_{endoleak2} = 30.8 s). The Δ time-to-peak value for the endoleak was 17.3 s. The patient underwent transarterial coil embolization of the aneurysm sac using 2D-3D image fusion as guidance during the procedure.

These two cases are presented to illustrate the technique described in the protocol section. Patients who underwent d-CTA imaging had potential endoleak (Patient selection). Prior image review was done to personalize individual scans such as higher kV than average for patients with a higher body-mass index (BMI), longer acquisition for possible type II endoleak (Patient II), shorter for Patient I with possible type I endoleak. Appropriate kV selection is crucial in ensuring adequate image quality; too low kV can result in suboptimal images (**Figure 9A**). The timing of the scans was made according to the step 2.4 of the protocol; this is an essential part because later launched acquisitions result in timing error and may influence qualitative analysis (**Figure 9B**). Image analysis was done in the dedicated software using the Dynamic Angio preset (**Figure 1** and **Figure 2**). The images were analyzed both qualitatively and quantitatively (**Figure 5-Figure 8**). Intra-operative image fusion was used to guide the intervention. The hybrid OR workstation aligned the fluoroscopic images with d-CTA images (**Figure 4**), as mentioned in step 4 of the protocol.

FIGURE AND TABLE LEGENDS:

Figure 1: Dynamic CTA scan opened with CT dynamic angio protocol. (A, B, C) The sagittal, axial, and coronal plane reconstructions aligned together. (D, E) Reconstructed images of a patient after a fenestrated-EVAR. The Blue arrow on the right shows the dynamic scans that are used for the review. The green arrow on the left shows the motion correction function (align body). This step is the initial when reviewing images. The white arrow on the left shows the timeline of the total scans, which can be changed manually or played continuously using the "watch" function. ROIs for TAC curves can be selected using the "TAC" function (yellow arrow).

Figure 2: Example of a TAC analysis in a patient with a type II endoleak from a lumbar artery as inflow. (A) The selected ROI (yellow above the stent-graft (ROI_{aorta}), green inside the aneurysm sac where endoleak is visualized ($ROI_{endoleak}$)). (B) This image demonstrates the generated time-attenuation curves for the selected ROIs in panel A. Time difference between aortic and endoleak curves in reaching peak Hounsfield unit is recorded (Δ time to peak value - marked with white)

Figure 3: Layout of the workstation in the hybrid OR to align the biplanar fluoroscopy images with the 3D dynamic scan (2D-3D image fusion). Yellow arrows highlight the wires inside the aorta, blue arrows show the inferior portion of the stent graft. Panel on the right is to manually modify the automatic alignment: visualization of fluoroscopic and d-CTA imaging, different image selection, fine modification of alignment, accepting the alignment. Additional measurements and annotations can be made using the blue box on the right panel.

Figure 4: Image of the overlaid markers on the real-time fluoroscopic image during coil embolization. The patient had a previous chimney-EVAR and a subsequent Ia gutter endoleak which was treated *via* coil embolization. Yellow arrows highlight the coil. Purple color is the marked endoleak cavity inside the deployed coils. Green circle indicates the fenestration of the implanted stent graft, horizontal green and blue lines are entrance for gutters next to the endoleak, and orange marks the top of the chimney graft.

Figure 5: An image of the 82-year-old male patient referred after an EVAR with possible type I or type II endoleak based on conventional CTA imaging. Sequentially imaged axial and sagittal plane scans are shown in the highlighted timepoint of the scan (the left top corner indicates the timepoint in seconds). A dashed yellow line marks the level of the axial images. The yellow arrow shows the contrast enhancement in the anterior margin of the stent-graft above the aneurysm sac, demonstrating a type Ia endoleak.

Figure 6: Time attenuation curve analysis of the patient shown in Figure 5. Selected ROIs are shown in (A) and (C) axial scans (aortic ROI at the top of the graft with orange and endoleak ROI at the level of contrast enhancement outside the graft). (B) is the TAC corresponding with the selected ROIs. The white box highlights the time to peak values for each region: $ROI_{3=aorta}$ and $ROI_{2=endoleak}$). The borders of the Δ time to peak value are shown with white dashed lines. The time interval between the two lines is the Δ time to peak value, which was 3.2 s. The short difference between peak values corresponds with type I endoleak.

Figure 7: Sequentially imaged, reconstructed axial and sagittal plane images of a 62-year-old male patient with a suspected type II endoleak. Each time point of the scan is shown in a separate panel (timepoints are shown in the top left corner). The dashed yellow line on the first sagittal image demonstrates the level of the axial images. Dynamic CTA showed sac enlargement with a type II endoleak from bilateral lumbar arteries at the level of the L3 vertebra (blue arrows). Endoleak is highlighted with yellow arrows. Time-resolved sagittal images demonstrate the downward flow inside the aneurysm sac from the level of the L3 lumbar vertebra.

Figure 8: Time attenuation curve for the type II endoleak. (A) The yellow circle shows the ROI for the aortic enhancement curve, green shows the ROI for the endoleak enhancement curve at the level of the L3 vertebra, and orange shows it at the level of the L4 vertebra. **(B)** Corresponding analysis of the curves showed a delayed Δ time to peak value for the endoleak (17.3 s) and a more delayed peak for the green region, demonstrating the downward flow. This confirms the presence of a type II endoleak.

Figure 9: This image shows the pitfalls of dynamic CTA image acquisition. (A) A scan was done at 70 kV for a patient with a BMI of 37.4. A high BMI value requires higher radiation exposure for acquiring acceptable images. **(B)** A timing error of a dynamic CTA. This scan was triggered later, and the aortic curve was already at the peak enhancement point when the acquisition started. The time attenuation curve shows the time to peak value at 0.2 s above the stent graft (corresponding ROI_{aorta} shown in **C**). TAC can be used to calculate Δ time to peak value even in these cases as well.

Table 1: Parameters of a customized d-CTA endoleak protocol. *Body-mass index for Patient I and II were 26.1 and 21.4 m²/kg.

DISCUSSION:

Dynamic, time-resolved CTA is an additional tool in the aortic imaging armamentarium. This technique can accurately diagnose endoleaks after EVAR, including identification of inflow/target vessels⁴.

Third-generation CT scanners with bidirectional table movement capability can provide dynamic acquisition mode with better temporal sampling along the time-attenuation curve⁶. To achieve the highest accuracy in the protocol it is critical to personalize image acquisition: review previously existing imaging set scan parameters according to patient requirement (high BMI – higher kV, cover the whole endograft with the scan, distribute scans based on suspected endoleak) and time the acquisition to cover aortic and endoleak enhancement curves (badly timed scan is shown in **Figure 9B**). An iodinated contrast agent with 320 mg of Iodine/mL was used in this study. While other contrast agents with lower iodine concentration may be used using this d-CTA protocol, increasing the contrast injection rate or volume might be necessary to achieve at least ~500 HU in the aortic region of interest.

Lower kV imaging comes at its own cost, especially in patients with higher BMI, as illustrated in **Figure 9A**. Advanced image reconstruction techniques using model-based, statistical methods

may help with improving image quality at lower radiation doses, especially during d-CTA imaging. Mistiming a scan can misrepresent quantitative data along the time attenuation curve (**Figure 9B**). Although such dynamic imaging techniques can be implemented in most third-generation CT scanners, a learning curve is associated with image acquisition, reconstruction, and post-processing time-resolved datasets.

The apparent roadblock for routine adoption of such dynamic, time-resolved CT imaging techniques concerns radiation and contrast exposure. While the amount of contrast injected is equivalent to triphasic CT imaging, the additional radiation exposure can be mitigated by lowering kV, selecting relevant scan range, and utilizing advanced iterative reconstruction techniques. Recent studies have shown that dynamic CTA can be performed without additional radiation exposure than conventional triphasic CTA^{5,10-12}. Minimizing radiation exposure of patients in EVAR surveillance is shown to be an essential and non-negligible factor¹³. This can be relevant in further CTA scan optimization to reduce scan numbers and subsequent radiation exposure without losing diagnostic accuracy¹⁴. Scan range is another crucial aspect that can be a limitation when using d-CTA; in our experience, 33 cm is the maximum length covered. Koike et al. using their different scanner and smaller scan range, published their approach to overcoming this limitation with promising results¹¹.

A previous study compared the accuracy of conventional and dynamic CTA and their impact on the number of digital subtraction angiographies during endoleak treatment⁵. Dynamic CTA has shown better endoleak diagnosing capability than conventional triphasic CTA⁵. According to recent papers, traditional CTA surveillance after EVAR may misdiagnose type II endoleaks, and multiple failed treatment attempts should raise suspicion for a different type of endoleaks¹⁰. The use of quantitative and qualitative image analysis from d-CTA may help overcome the limitation of diagnosing such misdiagnosed/occult endoleaks using conventional techniques¹⁵.

Image post-processing involves reviewing time-resolved dynamic CTA images and 2D-3D image fusion, typically taking ~5-10 min. Inaccuracies during image fusion may arise from the following factors: imperfect alignment of stent-graft from d-CTA with fluoroscopy, patient movement during the intervention, deformation of the aorta with stiff wires/devices. Further automation of image fusion techniques and workflow is required for better, seam-less intra-operative image guidance.

In our experience, d-CTA imaging has also been shown to provide additional image-fusion guidance during endoleak treatment⁶. Such dynamic time-resolved imaging can also be helpful in future imaging of other dynamic disease processes such as aortic dissection, peripheral arterial disease, arteriovenous malformations, or intramural hematoma¹⁶⁻¹⁸.

ACKNOWLEDGMENTS:

The authors would like to acknowledge Danielle Jones (Clinical education specialist, Siemens Healthineers) and the entire CT technologist team at Houston Methodist DeBakey Heart and vascular center to support imaging protocols.

DISCLOSURES:

ABL receives research support from Siemens Medical Solutions USA Inc., Malvern, PA. PC is a senior staff scientist at Siemens Medical Solutions USA Inc., Malvern, PA. Marton Berczeli is supported by Semmelweis University's scholarship: "Kiegészítő Kutatási Kiválósági Ösztöndíj" EFOP-3.6.3- VEKOP-16-2017-00009.

REFERENCES:

1. Lederle, F. A. et al. Open versus endovascular repair of abdominal aortic aneurysm. *New England Journal of Medicine*. **380** (22), 2126-2135 (2019).
2. De Bruin, J. L. et al. Long-term outcome of open or endovascular repair of abdominal aortic aneurysm. *New England Journal of Medicine*. **362** (20), 1881-1889 (2010).
3. Chaikof, E. L. et al. The Society for Vascular Surgery practice guidelines on the care of patients with an abdominal aortic aneurysm. *Journal of Vascular Surgery*. **67** (1), 2-77 e72 (2018).
4. Sommer, W. H. et al. Time-resolved CT angiography for the detection and classification of endoleaks. *Radiology*. **263** (3), 917-926 (2012).
5. Hou, K. et al. Dynamic volumetric computed tomography angiography is a preferred method for unclassified endoleaks by conventional computed tomography angiography after endovascular aortic repair. *Journal of American Heart Association*. **8** (8), e012011 (2019).
6. Berczeli, M., Lumsden, A. B., Chang, S. M., Bavare, C. S., Chinnadurai, P. Dynamic, time-resolved computed tomography angiography technique to characterize aortic endoleak type, inflow and provide guidance for targeted treatment. *Journal of Endovascular Therapy*. 15266028211037986 (2021).
7. Hertault, A. et al. Impact of hybrid rooms with image fusion on radiation exposure during endovascular aortic repair. *European Journal of Vascular and Endovascular Surgery*. **48** (4), 382-390 (2014).
8. Maurel, B. et al. Techniques to reduce radiation and contrast volume during EVAR. *Journal of Cardiovascular Surgery (Torino)*. **55** (2 Suppl 1), 123-131 (2014).
9. Schulz, C. J., Bockler, D., Krisam, J., Geisbusch, P. Two-dimensional-three-dimensional registration for fusion imaging is noninferior to three-dimensional- three-dimensional registration in infrarenal endovascular aneurysm repair. *Journal of Vascular Surgery*. **70** (6), 2005-2013, (2019).
10. Madigan, M. C., Singh, M. J., Chaer, R. A., Al-Khoury, G. E., Makaroun, M. S. Occult type I or III endoleaks are a common cause of failure of type II endoleak treatment after endovascular aortic repair. *Journal of Vascular Surgery*. **69** (2), 432-439, (2019).
11. Koike, Y. et al. Dynamic volumetric CT angiography for the detection and classification of endoleaks: application of cine imaging using a 320-row CT scanner with 16-cm detectors. *Journal of Vascular and Interventional Radiology*. **25** (8), 1172-1180 e1171 (2014).
12. Macari, M. et al. Abdominal aortic aneurysm: Can the arterial phase at CT evaluation after endovascular repair be eliminated to reduce radiation dose? *Radiology*. **241** (3), 908-914, (2006).
13. Brambilla, M. et al. Cumulative radiation dose and radiation risk from medical imaging in patients subjected to endovascular aortic aneurysm repair. *La Radiologica Medica*. **120** (6), 563-570 (2015).
14. Buffa, V. et al. Dual-source dual-energy CT: dose reduction after endovascular abdominal aortic aneurysm repair. *La Radiologica Medica*. **119** (12), 934-941 (2014).

- 441 15. Apfalter, G. et al. Quantitative analysis of dynamic computed tomography angiography
442 for the detection of endoleaks after abdominal aorta aneurysm endovascular repair: A feasibility
443 study. *PLoS One*. **16**(1), e0245134 (2021).
- 444 16. Kinner, S. et al. Dynamic MR angiography in acute aortic dissection. *Journal of Magnetic*
445 *Resonance Imaging*. **42** (2), 505-514 (2015).
- 446 17. Buls, N. et al. Improving the diagnosis of peripheral arterial disease in below-the-knee
447 arteries by adding time-resolved CT scan series to conventional run-off CT angiography. First
448 experience with a 256-slice CT scanner. *European Journal of Radiology*. **110**, 136-141, (2019).
- 449 18. Grossberg, J. A., Howard, B. M., Saindane, A. M. The use of contrast-enhanced, time-
450 resolved magnetic resonance angiography in cerebrovascular pathology. *Neurosurgical Focus*. **47**
451 (6), E3 (2019).
- 452

Figure 1.

[Click here to access/download;Figure;Figure_1_syngovia_layout.tif](#)

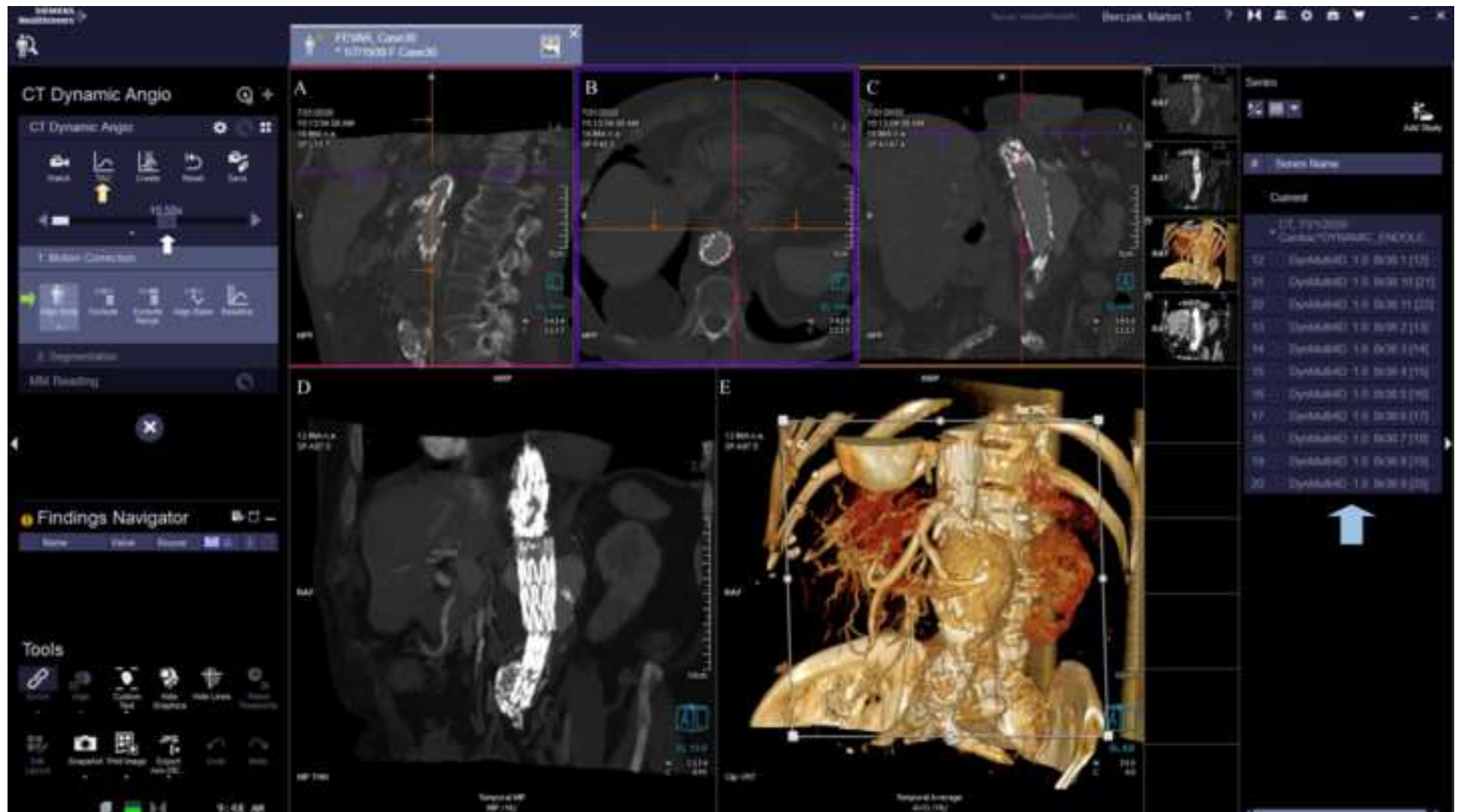


Figure 2.

[Click here to access/download;Figure;Figure_2_TAC_type_II_lumbar.tif](#)

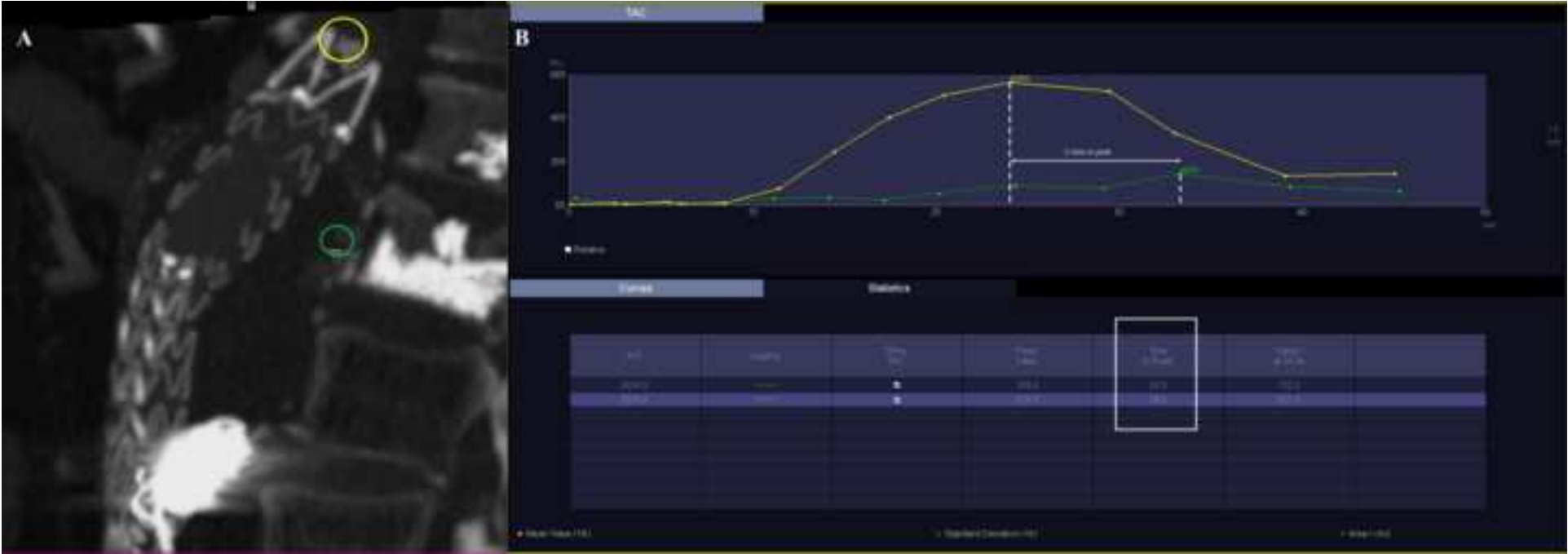


Figure 3.

[Click here to access/download;Figure;Figure_3_alignment.tif](#)

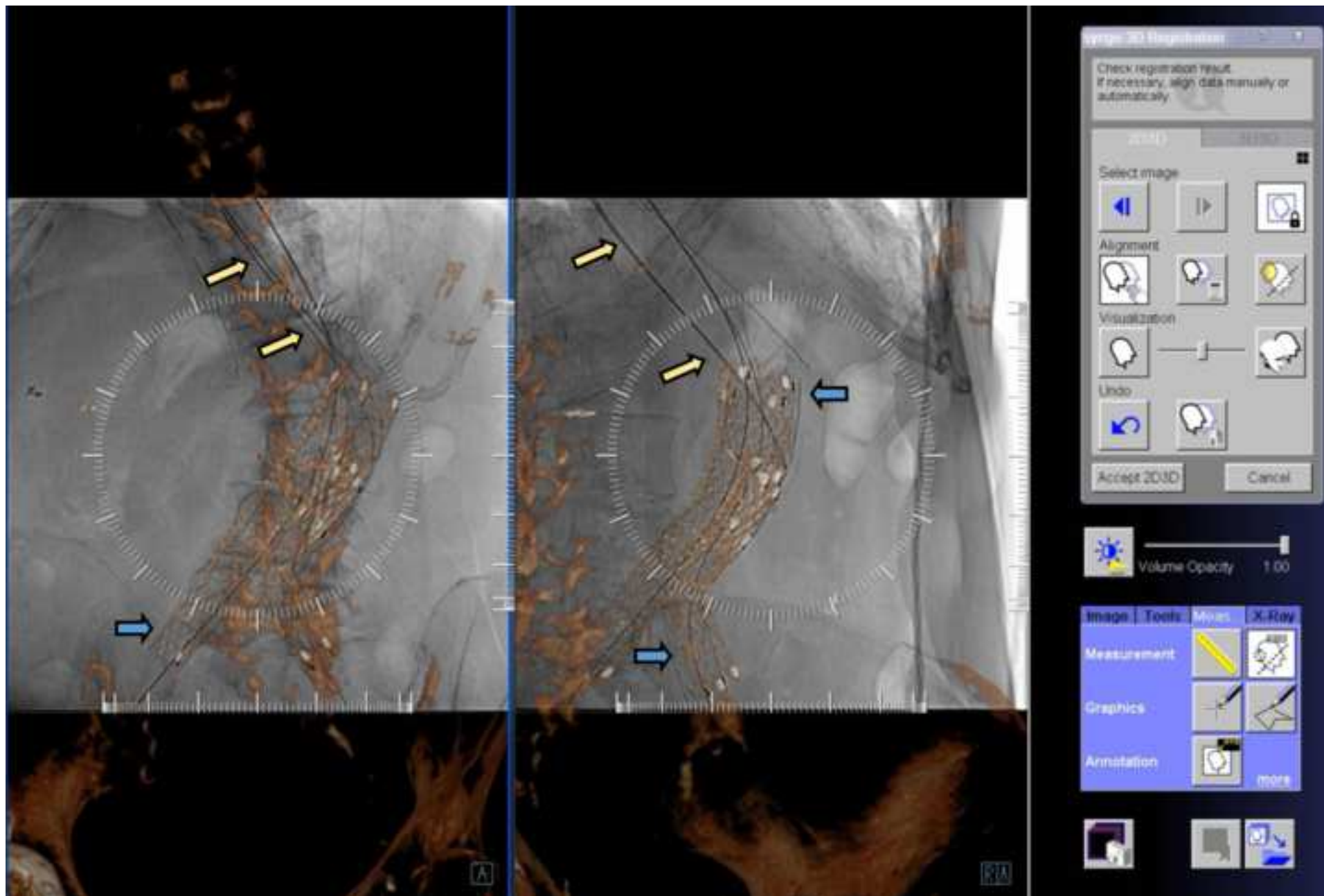
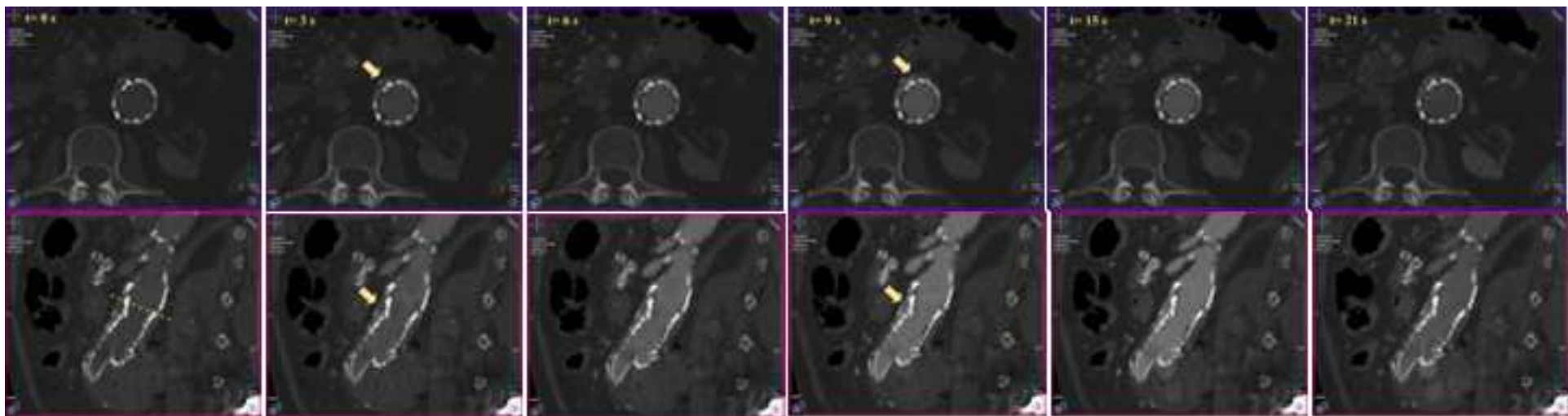




Figure 5.

[Click here to access/download;Figure;Figure_5_type_1a.tif](#)



[Click here to access/download;Figure;Figure_6_Typela_TAC.tiff](#)

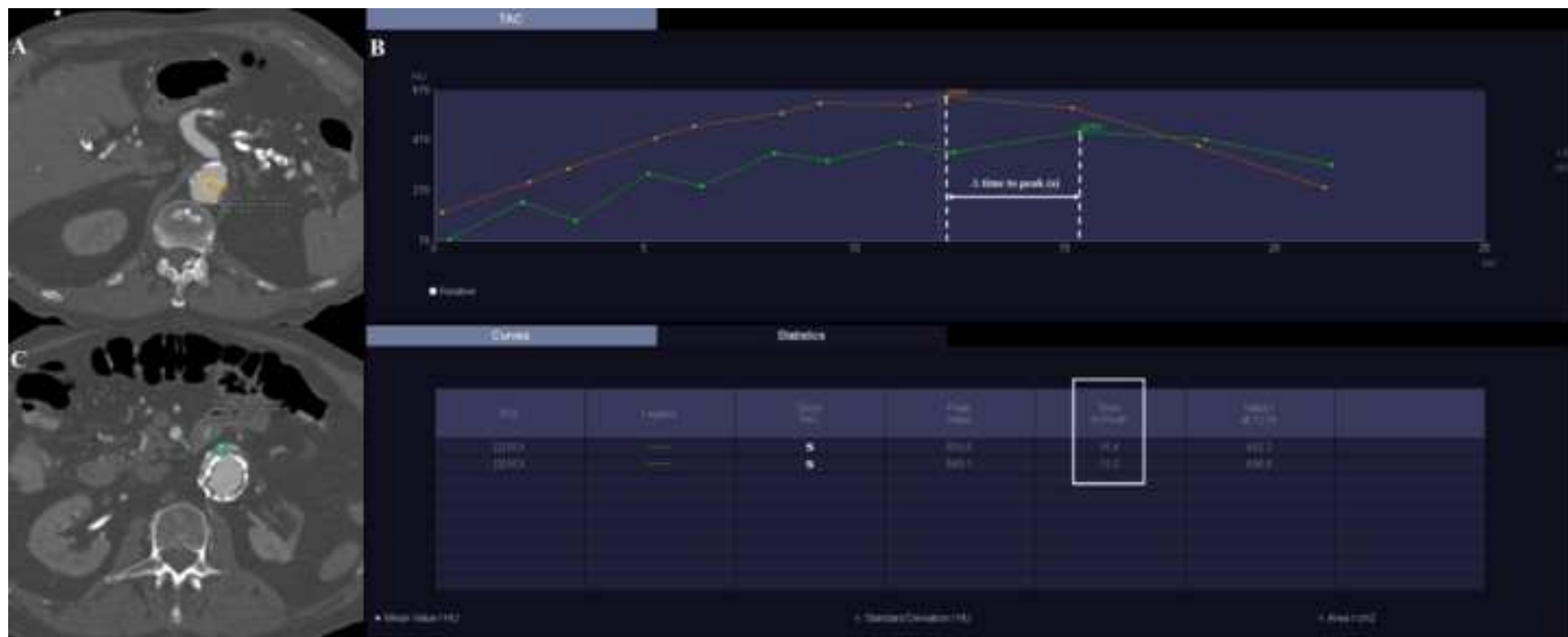


Figure 7.

[Click here to access/download;Figure;Figure_7_type_II_lumbar.tif](#)

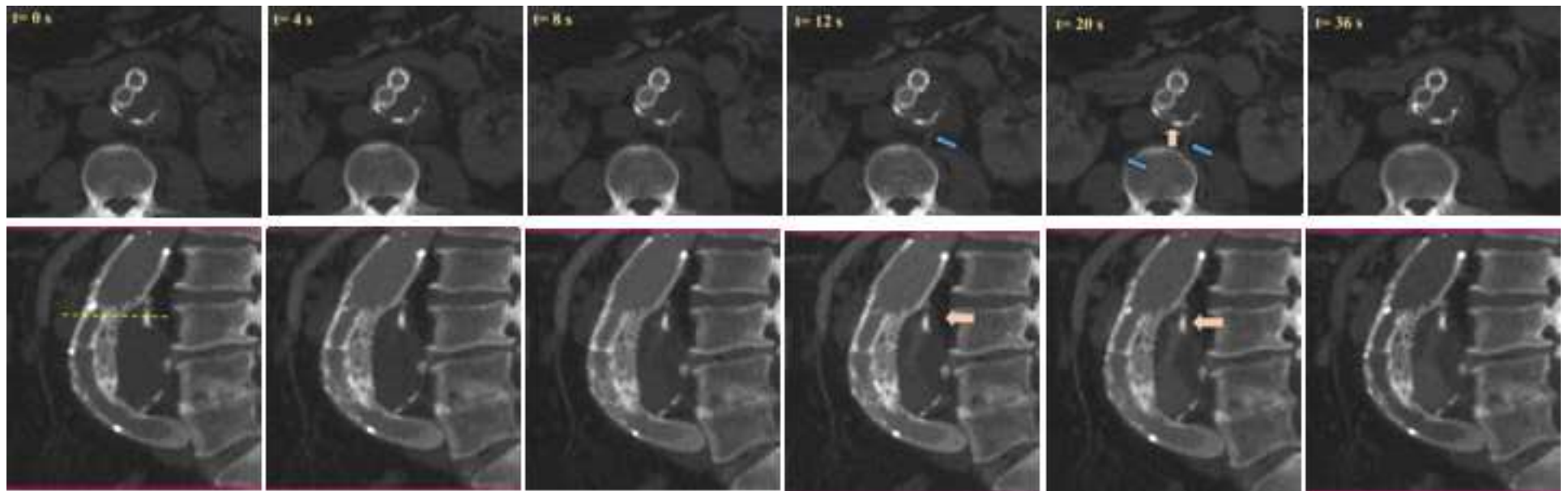


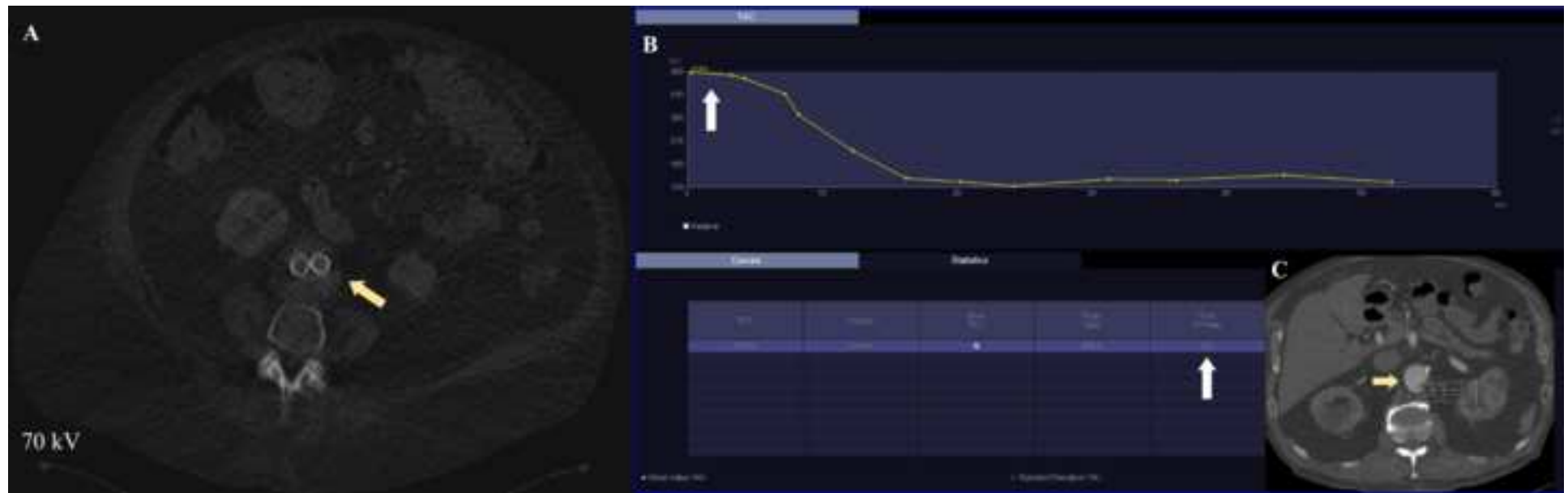
Figure 8.

[Click here to access/download;Figure;Figure_8_type_II_lumbar TAC.tiff](#)

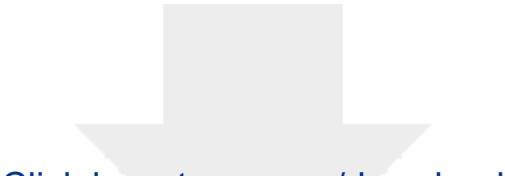


Figure 9.

[Click here to access/download;Figure;Figure_9_scan error.tif](#)



Protocol	DynMulti4D
Total number of volumes	11-13 scans - 2-4 scans @ every 1.5 s - 4 scans @ every 3 s - 2-4 scans @ every 4.5 s
Tube voltage	70-100 kV
Tube current	150 mAs
Rotation time	0.25 s
Scan duration	36±10 s
Slice thickness	0.7-1 mm
Contrast material volume	70-90 mL
Flow rate	3.5-4 mL/s
Saline flush	90-100 mL
Scan range (z-axis)	23-33 cm
Pitch	1
Reconstruction parameters	ADMIRE-3, Bv36 kernel
Dose-length product	593 (Patient I) and 445 Patient (II) mGy*cm



[Click here to access/download](#)

Table of Materials

[Material lists for dynamic-CT and image fusion.xlsx](#)



Dear Editor,

Thank you for your thoughts and comments on our manuscripts. We addressed them and modified our manuscript accordingly. We all hope you find our work meritable for publication. Regarding the videos we created multiple drafts and raw footages with video professionals that were uploaded to the shared folder.

Kind regards,
Marton Berczeli
Research fellow
Department of Cardiovascular Surgery
Houston Methodist Hospital

Voice over for dynamic CTA

Title:

Time-resolved, dynamic computed tomography angiography for characterization of aortic endoleaks and treatment guidance *via* 2D-3D fusion-imaging

Alan Lumsden:

Endoleak still remains the main challenge after endovascular aortic aneurysm repair and can be misdiagnosed. Unlike conventional CT imaging, dynamic, time-resolved CT-angiography has the advantage of visualizing the aneurysm sac during multiple time points after iodinated contrast injection. This technique helps identify all the vessels contributing to endoleak after EVAR and can be used for guiding endoleak treatment.

Marton Berczeli:

During dynamic CTA imaging, multiple scans are acquired after an intravenous bolus of iodinated contrast agent. To mitigate radiation exposure, the imaging is tailored to focus only in the region of previously implanted stent graft. Studies have shown that this modality has better diagnostic accuracy than conventional triphasic CTA imaging for endoleak.

Ponraj Chinnadurai:

Utilizing diagnostic images for intra-operative interventional guidance is not yet standard of care. Diagnosing and treating endoleak involves multiple 2D angiographic imaging at different C-arm angulations. This 3D dynamic CTA imaging can be combined with intra-operative 2D fluoroscopy using 2D/3D image fusion to facilitate interventional treatment, with limited radiation exposure and contrast agent usage.

Narrator:

The protocol starts with reviewing the patient's previous images. We load them to our DICOM file reviewer and check for potential endoleak on the available images. This can be informative to decide the scan range and temporal distribution during the image acquisition.

Representative results:

Presented here is a 76-year-old gentleman with type II diabetes, coronary artery disease and an endovascular aortic aneurysm repair in his medical history. The patient was referred to our institution based on sac enlargement and possible type II endoleak. After reviewing previous images, a possible type II endoleak was noted. A dynamic CT scan was performed at 70 kV acquiring 14 scans using 75 ml iodinated contrast material under 36 seconds. Careful review of the images demonstrated a contrast enhancement in the posterior segment of the aneurysm sac arising from bilateral L4 lumbar arteries. Quantitative analysis of the aortic and endoleak enhancement curve showed a 14.2 seconds time to peak value for the aortic and 27.5 seconds for the endoleak curve resulting in a 13.3 seconds delta time to peak value. These findings correlate with a type II endoleak.

Then for endoleak embolization the patient was taken into the hybrid OR. The scan with the highest diagnostic value was imported into the hybrid OR workstation and key landmarks as internal iliac artery orifice, iliolumbar arteries contributing to the endoleak were annotated with different colors.

After gaining femoral access and wire navigation into the aorta a 2D3D image fusion was performed and the two images were aligned.

A digital subtraction angiography was performed to confirm accurate alignment. Using the combination of a longer 5 Fr sheath, a microcatheter and a wire a microcatheter was positioned into the aneurysm sac and lumbar arteries and liquid embolization was performed. Completion images showed successful occlusion of the bilateral L4 lumbar arteries.

Conclusion:

Ponraj Chinnadurai:

To answer the underlying clinical question, imaging protocols can be customized to the individual patient, based on prior imaging findings. For suspected Type I endoleak, it is recommended to have more scans acquired during the earlier phase of the time-attenuation curve. For suspected type II endoleak, that appear later, it is recommended to have more scans during the later phase of the time-attenuation curve. If no prior imaging studies are available, scans can be distributed equally.

Marton Berczeli:

Using dynamic CT-angiography multiple inflow and outflow vessels can be identified this helps in better understanding of the endoleak and in targeting our treatment. This technique enables a quantitative approach to diagnosing aortic endoleaks (eg. Δ Time to peak can be used to differentiate type 1 vs 2 endoleaks). Using dynamic CT-fluoroscopy image fusion guidance for endoleak embolization, radiation exposure and contrast volume consumption can be reduced.

Alan Lumsden:

Dynamic, time-resolved CTA can adequately characterize endoleak types and inflow vessels. This is especially useful in complex endoleak cases when using the combination of qualitative and quantitative analysis we can distinguish between endoleak types. In our experience, d-CTA imaging has also been shown to provide additional image-fusion guidance during endoleak treatment. Such dynamic time-resolved CT imaging can also be helpful in future imaging of other dynamic disease processes such as aortic dissection, peripheral arterial disease, arteriovenous malformations, or intramural hematoma.

TITLE:

Time-Resolved, Dynamic Computed Tomography Angiography for Characterization of Aortic Endoleaks and Treatment Guidance *via* 2D-3D Fusion-Imaging

AUTHORS AND AFFILIATIONS:

Marton Berczeli^{1,2*}, Ponraj Chinnadurai^{1,3}, Su Min Chang⁴, Alan B. Lumsden¹

¹Department of Cardiovascular Surgery, Houston Methodist Hospital, Tx, USA

²Department of Vascular and Endovascular Surgery, Semmelweis University, Budapest, Hungary

³Advanced Therapies, Siemens Medical Solutions USA Inc., Malvern, PA, USA

⁴Department of Cardiology, Houston Methodist Hospital, Houston, Tx, USA

Email addresses of the authors:

Marton Berczeli marton.berczeli@gmail.com, mtberczeli@houstonmethodist.org

Ponraj Chinnadurai pchinnadurai@houstonmethodist.org

Su Min Chang smchang@houstonmethodist.org

Alan B. Lumsden ablumsden@houstonmethodist.org

*Email addresses of the corresponding author:

Marton Berczeli marton.berczeli@gmail.com, mtberczeli@houstonmethodist.org

KEYWORDS:

endovascular aneurysm repair, aortic endoleak, triphasic CT imaging, delayed CT imaging, dynamic CTA imaging, time-resolved CTA, EVAR, endoleak embolization, image fusion, post-EVAR surveillance

SUMMARY:

Dynamic computed tomography angiography (CTA) imaging provides additional diagnostic value in characterizing aortic endoleaks. This protocol describes a qualitative and quantitative approach using time-attenuation curve analysis to characterize endoleaks. The technique of integrating dynamic CTA imaging with fluoroscopy using 2D-3D image fusion is illustrated for better image guidance during treatment.

ABSTRACT:

In the United States, more than 80% of all abdominal aortic aneurysms are treated by endovascular aortic aneurysm repair (EVAR). The endovascular approach warrants good early results, but adequate follow-up imaging after EVAR is imperative to maintain long-term positive outcomes. Potential graft-related complications are graft migration, infection, fracture, and endoleaks, with the last one being the most common. The most frequently used imaging after EVAR is computed tomography angiography (CTA) and duplex ultrasound. Dynamic, time-resolved computed tomography angiography (d-CTA) is a reasonably new technique to characterize the endoleaks. Multiple scans are done sequentially around the endograft during acquisition that grants good visualization of the contrast passage and graft-related complications. This high diagnostic accuracy of d-CTA can be implemented into therapy *via* image fusion and

Commented [VB1]: Use the video JoVE_dCTA_draft3.mp4

reduce additional radiation and contrast material exposure.

This protocol describes the technical aspects of this modality: patient selection, preliminary image review, d-CTA scan acquisition, image processing, qualitative and quantitative endoleak characterization. The steps of integrating dynamic CTA into intra-operative fluoroscopy using 2D-3D fusion-imaging to facilitate targeted embolization are also demonstrated. In conclusion, time-resolved, dynamic CTA is an ideal modality for endoleak characterization with additional quantitative analysis. It can reduce radiation and iodinated contrast material exposure during endoleak treatment by guiding interventions.

INTRODUCTION:

Endovascular aortic aneurysm repair (EVAR) has shown superior early mortality results than open aortic repair¹. The approach is less invasive but may result in higher mid to long-term re-intervention rates due to endoleaks, graft migration, fracture². Hence better EVAR surveillance is critical to achieving good mid to long-term results.

Current guidelines suggest the routine use of duplex ultrasound and triphasic CTA³. Dynamic, time-resolved computed tomography angiography (d-CTA) is a relatively new modality used for EVAR surveillance⁴. During d-CTA, multiple scans are acquired in different time points along the time attenuation curve after contrast injection, hence the term time-resolved imaging. This approach has shown better accuracy in characterizing endoleaks after EVAR than conventional CTA⁵. An advantage of time-resolved acquisition is the ability to quantitatively analyze the Hounsfield unit changes in a selected region of interest (ROI)⁶.

The additional benefit of accurately characterizing endoleaks with d-CTA is that the scan can be used for image fusion during interventions, potentially minimizing the need for further diagnostic angiography. Image fusion is a method when previously acquired images are overlaid onto real-time fluoroscopy images to guide endovascular procedures and subsequently reduce contrast agent consumption and radiation exposure^{7,8}. Image fusion in the hybrid operating room (OR) using a 3D dynamic CTA scan can be achieved by two approaches: (1) 3D-3D image fusion: where 3D d-CTA is fused with intraoperatively acquired non-contrast cone-beam CT images, (2) 2D-3D image fusion, where 3D d-CTA is fused with biplanar (anteroposterior and lateral) fluoroscopic images. 2D-3D image fusion approach has been shown to significantly lower the radiation compared with 3D-3D technique⁹.

This protocol describes the technical and practical aspects of dynamic CTA imaging for endoleak characterization and introduces 2D-3D image fusion approach with d-CTA for intra-operative image guidance.

PROTOCOL:

This protocol follows the ethical standards of the national research committee and with the 1964 Helsinki declaration. This protocol is approved by Houston Methodist Research Institute.

1. Patient selection and prior image review

NOTE: Dynamic CTA imaging should be considered as a follow-up imaging modality in patients with increasing aneurysm size and endoleak after stent-graft implantation, persistent endoleak after interventions, or in patients with increasing aneurysms sac size without demonstrable endoleak. Like conventional CT imaging, this technique involves iodinated contrast injection that may be relatively contraindicated in patients with severe renal failure.

1.1. Before starting the actual scan, review the prior imaging studies for the presence of endoleak and stent-graft type.

NOTE: This can provide information to decide the scan range and temporal distribution during the image acquisition. The most commonly available imaging is the conventional CTA scans with bi-(non-contrast scan and arterial scan) or triple phase (non-contrast scan, arterial scan and delayed scan).

2. d-CTA Image acquisition

2.1. Position the patient in supine position on the CT scanner table.

2.2. Gain the peripheral venous access.

NOTE: Ensure that access is gained by visualizing the venous back bleeding.

2.3. Perform **topogram** and **non-contrast CT image acquisition** using Sn-100 Tin filter (see **Table of Materials**) to reduce the radiation exposure and for the region of interest selection in the d-CTA scan.

NOTE: After the non-contrast scan, the location of the endograft will be visible. Place the region of interest just above the endograft.

2.4. Perform timing bolus⁶ to check the contrast arrival time by placing a region of interest above the stent-graft in the abdominal aorta.

2.4.1. Inject 10-20 mL of the contrast (see **Table of Materials**) through the peripheral venous access, followed by 50 mL of saline injection at a 3.5–4 mL/min flow rate. Acquire timing bolus scan.

NOTE: Contrast arrival is recorded by the CT scanner (see **Table of Materials**) based on Hounsfield unit change inside the aorta⁶.

2.5. By selecting the DynMulti4D menu point in the pop-up “Cycle time window” plan the distribution and the number of scans based on the contrast arrival time from timing bolus and the findings from prior imaging studies.

Commented [BMT2]: Video: 0:13- 1:15

Commented [BMT3]: Video: 1:19 – 2:26

Commented [BMT4]: Video: 1:19

Commented [BMT5]: Video: 1:24 – 1:34

Commented [BMT6]: Video: 1:36 – 1:46

Commented [BMT7]: Video: 1: 46- 1:49

NOTE: If type I endoleak is suspected do more scans on the early phase of the contrast enhancement curve that is given by the timing bolus. If type II endoleak is suspected do more scans on the later phase.

2.5.1. For Type I endoleak, include more scans during the earlier phase of the time-attenuation curve (scan at every 1.5 s at the beginning and then every 3-4 s).

2.5.2. For type II endoleak, that appear later, include more scans during the later phase of the time-attenuation curve.

2.5.3. If no prior imaging studies are available, distribute the scans equally around the peak of time-attenuation curve.

2.6. Optimize imaging parameters including kV, scan range, etc. to reduce the radiation exposure. Use settings shown in **Table 1** for acquiring a dynamic scan with the CT scanner (see **Table of Materials**) used in this work.

2.7. Inject the contrast for d-CTA acquisition: 70-80 mL of the contrast material, followed by 100 mL of saline injections at a 3.5–4 mL/min flow rate through the peripheral access.

2.8. Start d-CTA image acquisition using the delay time based on the timing bolus described in step 2.4. Breath hold is not necessary during acquisition, given that the duration of d-CTA image acquisition ranges from 30–40 s.

2.9. Send acquired, reconstructed images to Picture Archiving and Communication System (PACS) for qualitative and quantitative review of time-resolved angiographic images. To do this select the data image and perform a mouse click on the bottom left side of the software.

3. Dynamic-CTA image analysis

3.1. Open the software (see **Table of Materials**) for reading the image. Search for the patient's name or identification number to find the acquired images. Select the acquired d-CTA images and process them using the **CT dynamic angio** workflow.

NOTE: The layout is shown in **Figure 1**.

3.2. Minimize respiratory motion artifacts between d-CTA images by selecting the dedicated software's **Align Body** motion correction menu item (**Figure 1**).

3.3. Qualitative analysis: Check axial slices of CT images when maximum opacification of aorta occurred, to interpret any obvious endoleak.

3.3.1. Then analyze scans in multiplanar reconstruction mode; if endoleak is suspected, focus on the endoleak and use the timescale shown in **Figure 1** to watch time-resolved images and

Commented [BMT8]: 2.6-2.7 : Video: 1:52 – 1:54
2.8.: Video 1:55-2:25

During the time period of 1:55-2:25 steps: 2.5.1, 2.5.2 and 2.5.3 can be mentioned as well

Commented [VB9]: Added here. Please check.

Commented [BMT10R9]: Thank you

Commented [BMT11]: Video: 2:26-4:36

Commented [BMT12]: Video: 2:26 – 3:23

Commented [BMT13]: Video 3:24 – 4:05

infer the source of endoleak.

3.4. Quantitative analysis: Click on the **time attenuation curve (TAC)** function shown in **Figure 1**. Select a region above the stent graft (ROI_{aorta}) and draw a circle using the TAC function, then select the endoleak (ROI_{endoleak}) region and draw a circle there as well.

NOTE: Target vessels can be selected (ROI_{target}) to determine the role of the vessel to the endoleak (inflow or outflow).

3.4.1. Analyze the acquired TAC (**Figure 2**) to determine the endoleak characteristics. Subtract the time to peak value of the endoleak and the aortic ROI curves to get the Δ time to peak value. This value can be used for endoleak analysis⁶.

3.5. After qualitative and quantitative analysis, infer the type and source of endoleak.

NOTE: Type I endoleaks appear as parallel contrast enhancement next to the graft, usually because of the inadequate sealing zone and have a shorter time difference between aortic and endoleak enhancement curve (Δ time to peak value) between aortic and endoleak ROI. Type II endoleaks are related to an inflow vessel with retrograde filling through collateral and have prolonged Δ time to peak value between aortic and endoleak ROI. Based on experience, a Δ time-to-peak value of higher than 4 s was not recorded for type I endoleaks.

4. Intra-operative image fusion guidance

4.1. Position the patient supine on the hybrid operating room (OR) table.

4.2. Load the selected dynamic CTA scan that has the best visibility of the endoleak in the hybrid OR workstation. Manually annotate critical landmarks on the scan: renal arteries ostia, internal iliac arteries ostia, endoleak cavity, lumbar artery(ies), or inferior mesenteric artery.

4.3. Select 2D3D image fusion in the workstation and acquire an anteroposterior and an oblique fluoroscopic image of the patient using the 2D-3D image fusion workflow. For this, move the C-arm to the required angle(s) with the joystick on the operating table and step on the CINE acquisition pedal.

4.4. Electronically align the stent-graft with markers from the 3D dynamic CTA scan with the fluoroscopic images using automated image registration, followed by manual refinement if necessary (**Figure 3**) in the 3D post-processing workstation (Drag one images for manual alignment). Check and accept the **2D-3D image fusion** and **overlay** the markers from d-CTA on the real-time 2D fluoroscopic image (**Figure 4**).

4.5. Perform the endoleak embolization using the overlaid markers from d-CTA as guidance.

REPRESENTATIVE RESULTS:

Commented [BMT14]: The actual analysis was moved into the "results section" to 7:40- 8:53

Commented [BMT15]: Video: 4:05 – 4:33

Commented [BMT16]: This was also moved into the results section of the video.
Video: 8:54 – 9:21

Commented [BMT17]: Video: 4:35 – 5:51

Commented [BMT18]: Video: 5:52- 6:42

Commented [BMT19]: Video: 6:43 – 7:35

The dynamic imaging workflow in two patients is illustrated here.

Patient I

An 82-year-old male patient with chronic obstructive pulmonary disease and hypertension had a previous infrarenal EVAR (2016). In 2020 the patient was referred from an outside hospital for a possible type I or type II endoleak based on conventional CTA. and an adjunctive endoanchor placement in 2020 for type Ia endoleak. Dynamic CTA was performed that diagnosed a type Ia endoleak, and the patient underwent proximal zone ballooning plus received endoanchors to gain more sealing zone for the graft. After the intervention, a dynamic control CTA was performed, acquiring 12 scans under 21 s scan time with 90 kV using 85 mL iodinated contrast material. Qualitative analysis showed a persisting type Ia endoleak illustrated in **Figure 5**. Quantitative TAC analysis showed a 12.2 s time to peak value for ROI_{aorta} and a 15.4 sec to peak value for ROI_{endoleak} creating a 3.2 s time to a peak value (**Figure 6**). The patient received a fenestrated-EVAR; the procedure was done using 2D-3D image fusion during the procedure.

Patient II

A 62-year-old male patient with a medical history of obesity, stroke, renal insufficiency (creatinine: 2.02 mg/dL), hypertension, hyperlipidemia, and coronary artery disease. The patient received an infrarenal EVAR at an outside hospital in 2018. He was referred to our Institution for a possible type II endoleak on conventional CTA. Dynamic CTA was performed with acquiring 12 scans under 52 s at 100 kV using 70 mL iodinated contrast material. Sac enlargement with a type II endoleak was detected from bilateral L3 lumbar arteries as inflow vessels shown in **Figure 7**. Time attenuation curve analysis showed a 7.2 s time to peak value for ROI_{aorta} and 24.6 s for ROI_{endoleak} at the level of the L3 vertebra (**Figure 8**). An additional ROI was selected in the inferior portion of the sac, demonstrating the downward flow from the level of the bilateral lumbar arteries by the delayed time to a peak value (ROI_{endoleak2} = 30.8 s). The Δ time-to-peak value for the endoleak was 17.3 s. The patient underwent transarterial coil embolization of the aneurysm sac using 2D-3D image fusion as guidance during the procedure.

These two cases are presented to illustrate the technique described in the protocol section. Patients who underwent d-CTA imaging had potential endoleak (Patient selection). Prior image review was done to personalize individual scans such as higher kV than average for patients with a higher body-mass index (BMI), longer acquisition for possible type II endoleak (Patient II), shorter for Patient I with possible type I endoleak. Appropriate kV selection is crucial in ensuring adequate image quality; too low kV can result in suboptimal images (**Figure 9A**). The timing of the scans was made according to step 2.4 of the protocol; this is an essential part because later launched acquisitions result in timing error and may influence qualitative analysis (**Figure 9B**). Image analysis was done in the dedicated software using the Dynamic Angio preset (**Figure 1** and **Figure 2**). The images were analyzed both qualitatively and quantitatively (**Figure 5-8**). Intra-operative image fusion was used to guide the intervention. The hybrid OR workstation aligned the fluoroscopic images with d-CTA images (**Figure 4**), as mentioned in step 4 of the protocol.

FIGURE AND TABLE LEGENDS:

Figure 1: Dynamic CTA scan opened with CT dynamic angio protocol. (A, B, C) The sagittal, axial, and coronal plane reconstructions aligned together. **(D, E)** Reconstructed images of a patient after a fenestrated-EVAR. The Blue arrow on the right shows the dynamic scans that are used for the review. The green arrow on the left shows the motion correction function (align body). This step is the initial when reviewing images. The white arrow on the left shows the timeline of the total scans, which can be changed manually or played continuously using the "watch" function. ROIs for TAC curves can be selected using the "TAC" function (yellow arrow).

Figure 2: Example of a TAC analysis in a patient with a type II endoleak from a lumbar artery as inflow. (A) The selected ROI (yellow above the stent-graft (ROI_{aorta}), green inside the aneurysm sac where endoleak is visualized (ROI_{endoleak})). **(B)** This image demonstrates the generated time-attenuation curves for the selected ROIs in Fig. 2A. Time difference between aortic and endoleak curves in reaching peak Hounsfield unit is recorded (Δ time to peak value - marked with white)

Figure 3: Layout of the workstation in the hybrid OR to align the biplanar fluoroscopy images with the 3D dynamic scan (2D-3D image fusion). Yellow arrows highlight the wires inside the aorta, blue arrows show the inferior portion of the stent-graft. Panel on the right is to manually modify the automatic alignment: visualization of fluoroscopic and d-CTA imaging, different image selection, fine modification of alignment, accepting the alignment. Additional measurements and annotations can be made using the blue box on the right panel.

Figure 4: Image of the overlaid markers on the real-time fluoroscopic image during coil embolization. The patient had a previous chimney-EVAR and a subsequent Ia gutter endoleak which was treated *via* coil embolization. Yellow arrows highlight the coil. Purple color is the marked endoleak cavity with inside the deployed coils. Green circle indicates the fenestration of the implanted stent graft, horizontal green and blue lines are entrance for gutters next to the endoleak and orange marks the top of the chimney graft.

Figure 5: An image of the 82-year-old male patient referred after an EVAR with possible type I or type II endoleak based on conventional CTA imaging. Sequentially imaged axial and sagittal plane scans are shown in the highlighted timepoint of the scan (the left top corner indicates the timepoint in seconds). A dashed yellow line marks the level of the axial images. The yellow arrow shows the contrast enhancement in the anterior margin of the stent-graft above the aneurysm sac, demonstrating a type Ia endoleak.

Figure 6: Time attenuation curve analysis of the patient shown in Figure 5. Selected ROIs are shown in **(A)** and **(C)** axial scans (aortic ROI at the top of the graft with orange and endoleak ROI at the level of contrast enhancement outside the graft). **(B)** is the TAC corresponding with the selected ROIs. The white box highlights the time to peak values for each region: ROI_{3=aorta} and ROI_{2=endoleak}). The borders of the Δ time to peak value are shown with white dashed lines. The time interval between the two lines is the Δ time to peak value, which was 3.2 s. The short difference between peak values corresponds with type I endoleak.

Figure 7: Sequentially imaged, reconstructed axial and sagittal plane images of a 62-year-old

male patient with a suspected type II endoleak. Each time point of the scan is shown in a separate panel (timepoints are shown in the top left corner). The dashed yellow line on the first sagittal image demonstrates the level of the axial images. Dynamic CTA showed sac enlargement with a type II endoleak from bilateral lumbar arteries at the level of the L3 vertebra (blue arrows). Endoleak is highlighted with yellow arrows. Time-resolved sagittal images demonstrate the downward flow inside the aneurysm sac from the level of the L3 lumbar vertebra.

Figure 8: Time attenuation curve for the type II endoleak. (A) The yellow circle shows the ROI for aortic enhancement curve, green shows the ROI for endoleak enhancement curve at the level of the L3 vertebra, and orange shows it at the level of the L4 vertebra. (B) Corresponding analysis of the curves showed a delayed Δ time to peak value for the endoleak (17.3 s) and a more delayed peak for the green region, demonstrating the downward flow. This confirms the presence of a type II endoleak.

Figure 9: This image shows the pitfalls of dynamic CTA image acquisition. (A) A scan was done at 70 kV for a patient with a BMI of 37.4. A high BMI value requires higher radiation exposure for acquiring acceptable images. (B) A timing error of a dynamic CTA. This scan was triggered later, and the aortic curve was already at the peak enhancement point when the acquisition started. The time attenuation curve shows the time to peak value at 0.2 s above the stent-graft (corresponding ROI_{aorta} shown in C). TAC can be used to calculate Δ time to peak value even in these cases as well.

Table 1: Parameters of a customized d-CTA endoleak protocol. *Body-mass index for Patient I and II were 26.1 and 21.4 m²/kg.

DISCUSSION:

Dynamic, time-resolved CTA is an additional tool in the aortic imaging armamentarium. This technique can accurately diagnose endoleaks after EVAR, including identification of inflow/target vessels⁴.

Third-generation CT scanners with bidirectional table movement capability can provide dynamic acquisition mode with better temporal sampling along the time-attenuation curve⁶. Critical in the protocol to achieve the highest accuracy is to personalize image acquisition: review previously existing imaging set scan parameters according to patient requirement (high BMI – higher kV, cover the whole endograft with the scan, distribute scans based on suspected endoleak) and time the acquisition to cover aortic and endoleak enhancement curves (badly timed scan is shown in **Figure 9B**). An iodinated contrast agent with 320 mg of Iodine/mL was used in this study. While other contrast agents with lower iodine concentration may be used using this d-CTA protocol, increasing the contrast injection rate or volume might be necessary to achieve at least ~500 HU in the aortic region of interest.

Lower kV imaging comes at its own cost, especially in patients with higher BMI, as illustrated in **Figure 9A**. Advanced image reconstruction techniques using model-based, statistical methods may help with improving image quality at lower radiation doses, especially during d-CTA imaging.

Mistiming a scan can misrepresent quantitative data along the time attenuation curve (**Figure 9B**). Although such dynamic imaging techniques can be implemented in most third-generation CT scanners, a learning curve is associated with image acquisition, reconstruction, and post-processing time-resolved datasets.

The apparent roadblock for routine adoption of such dynamic, time-resolved CT imaging techniques concerns radiation and contrast exposure. While the amount of contrast injected is equivalent to triphasic CT imaging, the additional radiation exposure can be mitigated by lowering kV, selecting relevant scan range, and utilizing advanced iterative reconstruction techniques. Recent studies have shown that dynamic CTA can be performed without additional radiation exposure than conventional triphasic CTA^{5,10-12}. Minimizing radiation exposure of patients in EVAR surveillance is shown to be an essential and non-negligible factor¹³. This can be relevant in further CTA scan optimization to reduce scan numbers and subsequent radiation exposure without losing diagnostic accuracy¹⁴. Scan range is another crucial aspect that can be a limitation when using d-CTA; in our experience, 33 cm is the maximum length covered. Koike et al. using their different scanner and smaller scan range published their approach to overcoming this limitation with promising results¹¹.

A previous study compared the accuracy of conventional and dynamic CTA and their impact on the number of digital subtraction angiographies during endoleak treatment⁵. Dynamic CTA has shown better endoleak diagnosing capability than conventional triphasic CTA⁵. According to recent papers, traditional CTA surveillance after EVAR may misdiagnose type II endoleaks, and multiple failed treatment attempts should raise suspicion for a different type of endoleaks¹⁰. The use of quantitative and qualitative image analysis from d-CTA may help overcome the limitation of diagnosing such misdiagnosed/occult endoleaks using conventional techniques¹⁵.

Image post-processing involves reviewing time-resolved dynamic CTA images and 2D-3D image fusion, typically taking ~5-10 min. Inaccuracies during image fusion may arise from the following factors: imperfect alignment of stent-graft from d-CTA with fluoroscopy, patient movement during the intervention, deformation of the aorta with stiff wires/devices. Further automation of image fusion techniques and workflow is required for better, seam-less intra-operative image guidance.

In our experience, d-CTA imaging has also been shown to provide additional image-fusion guidance during endoleak treatment⁶. Such dynamic time-resolved imaging can also be helpful in future imaging of other dynamic disease processes such as aortic dissection, peripheral arterial disease, arteriovenous malformations, or intramural hematoma¹⁶⁻¹⁸.

ACKNOWLEDGMENTS:

The authors would like to acknowledge Danielle Jones (Clinical education specialist, Siemens Healthineers) and the entire CT technologist team at Houston Methodist DeBakey Heart and vascular center to support imaging protocols.

DISCLOSURES:

ABL receives research support from Siemens Medical Solutions USA Inc., Malvern, PA. PC is a senior staff scientist at Siemens Medical Solutions USA Inc., Malvern, PA. Marton Berczeli is supported by Semmelweis University's scholarship: "Kiegészítő Kutatási Kiválósági Ösztöndíj" EFOP-3.6.3- VEKOP-16-2017-00009.

REFERENCES:

1. Lederle, F. A. et al. Open versus Endovascular Repair of Abdominal Aortic Aneurysm. *New England Journal of Medicine*. 380 (22), 2126-2135 (2019).
2. De Bruin, J. L. et al. Long-term outcome of open or endovascular repair of abdominal aortic aneurysm. *New England Journal of Medicine*. 362 (20), 1881-1889, (2010).
3. Chaikof, E. L. et al. The Society for Vascular Surgery practice guidelines on the care of patients with an abdominal aortic aneurysm. *Journal of Vascular Surgery*. 67 (1), 2-77 e72, (2018).
4. Sommer, W. H. et al. Time-resolved CT angiography for the detection and classification of endoleaks. *Radiology*. 263 (3), 917-926, (2012).
5. Hou, K. et al. Dynamic Volumetric Computed Tomography Angiography Is a Preferred Method for Unclassified Endoleaks by Conventional Computed Tomography Angiography After Endovascular Aortic Repair. *Journal of American Heart Association*. 8 (8), e012011, (2019).
6. Berczeli M, Lumsden AB, Chang SM, Bavare CS, Chinnadurai P. Dynamic, Time-Resolved Computed Tomography Angiography Technique to Characterize Aortic Endoleak Type, Inflow and Provide Guidance for Targeted Treatment [published online ahead of print, 2021 Aug 13]. *Journal of Endovascular Therapy*. 2021;15266028211037986. doi:10.1177/15266028211037986
7. Hertault, A. et al. Impact of hybrid rooms with image fusion on radiation exposure during endovascular aortic repair. *European Journal of Vascular and Endovascular Surgery*. 48 (4), 382-390, (2014).
8. Maurel, B. et al. Techniques to reduce radiation and contrast volume during EVAR. *Journal of Cardiovascular Surgery (Torino)*. 55 (2 Suppl 1), 123-131, (2014).
9. Schulz, C. J., Bockler, D., Krisam, J. & Geisbusch, P. Two-dimensional-three-dimensional registration for fusion imaging is noninferior to three-dimensional- three-dimensional registration in infrarenal endovascular aneurysm repair. *Journal of Vascular Surgery*. 70 (6), 2005-2013, (2019).
10. Madigan, M. C., Singh, M. J., Chaer, R. A., Al-Khoury, G. E. & Makaroun, M. S. Occult type I or III endoleaks are a common cause of failure of type II endoleak treatment after endovascular aortic repair. *Journal of Vascular Surgery*. 69 (2), 432-439, (2019).
11. Koike, Y. et al. Dynamic volumetric CT angiography for the detection and classification of endoleaks: application of cine imaging using a 320-row CT scanner with 16-cm detectors. *Journal of Vascular and Interventional Radiology*. 25 (8), 1172-1180 e1171, (2014).
12. Macari, M. et al. Abdominal aortic aneurysm: can the arterial phase at CT evaluation after endovascular repair be eliminated to reduce radiation dose? *Radiology*. 241 (3), 908-914, (2006).
13. Brambilla M, Cerini P, Lizio D, Vigna L, Carrierio A, Fossaceca R. Cumulative radiation dose and radiation risk from medical imaging in patients subjected to endovascular aortic aneurysm repair. *La Radiologica Medica*. 2015;120(6):563-570. doi:10.1007/s11547-014-0485-x
14. Buffa V, Solazzo A, D'Auria V, et al. Dual-source dual-energy CT: dose reduction after endovascular abdominal aortic aneurysm repair. *La Radiologica Medica*. 2014;119(12):934-941. doi:10.1007/s11547-014-0420-1

- 441 15. Apfalter G, Lavra F, Schoepf UJ, et al. Quantitative analysis of dynamic computed
442 tomography angiography for the detection of endoleaks after abdominal aorta aneurysm
443 endovascular repair: A feasibility study. *PLoS One*. 2021;16(1):e0245134. Published 2021 Jan 7.
444 doi:10.1371/journal.pone.0245134
- 445 16. Kinner, S. et al. Dynamic MR angiography in acute aortic dissection. *Journal of Magnetic*
446 *Resonance Imaging*. 42 (2), 505-514, (2015).
- 447 17. Buls, N. et al. Improving the diagnosis of peripheral arterial disease in below-the-knee
448 arteries by adding time-resolved CT scan series to conventional run-off CT angiography. First
449 experience with a 256-slice CT scanner. *European Journal of Radiology*. 110 136-141, (2019).
- 450 18. Grossberg, J. A., Howard, B. M. & Saindane, A. M. The use of contrast-enhanced, time-
451 resolved magnetic resonance angiography in cerebrovascular pathology. *Neurosurgical Focus*. 47
452 (6), E3, (2019).
- 453